



Review

# Recent Advances in Porous 3D Cellulose Aerogels for Tissue Engineering Applications: A Review

Ali Mirtaghavi<sup>1</sup>, Jikui Luo<sup>1,2,\*</sup>  and Rajendran Muthuraj<sup>1,\*</sup>

<sup>1</sup> Institute for Materials Research and Innovation, University of Bolton, Deane Road, Bolton BL3 5AB, UK; am26mpo@bolton.ac.uk

<sup>2</sup> Key Laboratory of Advanced Micro/Nano Electronic Devices & Smart Systems of Zhejiang, College of Information Science and Electronic Engineering, Zhejiang University, Hangzhou 310027, China

\* Correspondence: J.luo@bolton.ac.uk (J.L.); rajendranpolychem@gmail.com (R.M.)

Received: 16 September 2020; Accepted: 15 October 2020; Published: 19 October 2020



**Abstract:** Current approaches in developing porous 3D scaffolds face various challenges, such as failure of mimicking extracellular matrix (ECM) native building blocks, non-sustainable scaffold fabrication techniques, and lack of functionality. Polysaccharides and proteins are sustainable, inexpensive, biodegradable, and biocompatible, with structural similarities to the ECM. As a result, 3D-structured cellulose (e.g., cellulose nanofibrils, nanocrystals and bacterial nanocellulose)-based aerogels with high porosity and interconnected pores are ideal materials for biomedical applications. Such 3D scaffolds can be prepared using a green, scalable, and cost-effective freeze-drying technique. The physicochemical, mechanical, and biological characteristics of the cellulose can be improved by incorporation of proteins and other polysaccharides. This review will focus on recent developments related to the cellulose-based 3D aerogels prepared by sustainable freeze-drying methods for tissue engineering applications. We will also provide an overview of the scaffold development criteria; parameters that influenced the aerogel production by freeze-drying; and in vitro and in vivo studies of the cellulose-based porous 3D aerogel scaffolds. These efforts could potentially help to expand the role of cellulose-based 3D scaffolds as next-generation biomaterials.

**Keywords:** sustainable; 3D scaffolds; polysaccharides and proteins; cellulose; tissue engineering

## 1. Introduction

Injuries, trauma, and diseases have led to severe degeneration of tissues in various human organs; therefore, it has always been of interest to facilitate the repair or regenerate of such damaged tissues. The conventional treatments typically focus on transplanting tissue from one site to another, whether from the same patient (autograph), from another donor (allograft), or from another species (xenograft). These treatments have been revolutionary and lifesaving, yet they lack scientific and clinical validations such as donor site morbidity, pathogen transmission, and immune response rejection, and they can be expensive [1,2]. To this end, tissue engineering provides new hopes for the treatment of damaged tissues and organs by regenerating the damaged ones instead of replacing them with tissues from others. Organs can potentially be regrown through the development of biological substitutes and are an interdisciplinary scientific field of research [3].

Tissue engineering strongly relies on the use of porous structures (the so-called “scaffolds”) that can provide a template for tissue formation and are able to maintain an environment to supply nutrients and carry metabolites for cells. Scaffolds can also enhance matrix deposition and remove end-product waste of cell metabolites [4]. The major function of a scaffold is to offer alternative features found naturally within the extracellular matrix (ECM) needed for native cells to function. These scaffolds must provide structural similarities to the ECM by offering a highly porous (with interconnected pores) 3-dimensional

(3D) environment with an adequate mechanical resilience for tissues and display biological activity that can induce cell migration, attachment and differentiation [5]. Preparation of functional scaffolds using synthetic polymers has been widely studied, however, there are some limitations associated with these materials, such as biocompatibility, biodegradability, sustainability and environmentally friendliness. Therefore, renewable polymers (e.g., proteins and polysaccharides) have been studied as alternative to prepare such scaffolds with facile and cost-effective methods [6]. Table 1 highlights some of the most studied porous scaffolds prepared by using both synthetic as well as natural polymers. The use of biopolymer-based porous 3D scaffolds has been receiving a great deal of attention. Moreover, nanocellulose has emerged as an attractive candidate in the fabrication of aerogels due to its excellent mechanical properties, biocompatibility, highly porous 3D architecture and high specific surface area. Nanocellulose can be categorized into three main types; long, flexible cellulose nanofibers, short; rigid cellulose nanocrystals; and highly crystalline, pure bacterial nanocellulose [7]. In this context, this review aims to provide an overview of the current advancement in the development of highly porous 3D aerogels for tissue engineering applications.

**Table 1.** Different scaffolds with different porosities were used for different cell activities.

| Scaffold Application                     | Type of Cell Incorporated In Vivo   | Scaffold Type                           | Fabrication Technique                          | Pore Size (µm) | Porosity (%) | Reference |
|--|---|---|--|----------------|--------------|-----------|
| Soft tissue regeneration                 | chicken embryo fibroblast   | Cellulose-TiO <sub>2</sub> -Ag          | Freeze-drying                                  | -              | 96           | [8]       |
| Adipogenesis                             | Murine embryonic stem cells (rat BMCs)  | - PCL                                   | Electrospinning                                | 6–70           | 88           | [9,10]    |
|  |   | - Silk gland fibroin from nonmulberry   | Freeze-drying                                  | 90–110         | 97           |           |
| Chondrogenesis (cartilage regeneration)  | - Human ASCs<br>- Porcine chondrocytes<br>- Rabbit MSCs<br>- Porcine BMSCs                        | - PCL                                   | Centrifugation method                          | 70–120         | 95           | [11–15]   |
|  |   | - CNF-gelatin-chitosan                  | Freeze-drying                                  | 190            | 80           |           |
|  |   | - Cellulose/PLA                         | Freeze-gelation                                | 200            | 95           |           |
|  |   | - PEG-chitosan<br>- PCL, PLGA           | Freeze drying and electrospinning              | 200–500<br>750 | 30<br>59     |           |
| Hepatogenesis (bone marrow regeneration) | Human ASCs<br>Rat bone marrow stem cells  | - PLGA                                  | Low-temperature deposition                     | 120–200        | -            | [11]      |
|  |   | - c-PLGA                                |  | 150–350        | 85           |           |
| Osteogenesis                             | - In vivo rat implantation<br>- hMSC<br>- In vivo mice implantation<br>- fetal bovine osteoblasts | - HA-BMPs                               | Hydrothermal treatment<br>Extrusion deposition | 300–400        | -            | [12–14]   |
|  |   | - Coralline HA                          |  | 200            | 75           |           |
|  |   | - β-tricalcium phosphate, natural coral |  | 2–100          | 75           |           |
|  |   | - PCL                                   |  | 350            | 65           |           |
| Skin Regeneration                        | - Primary rat osteoblasts<br>- Guinea pig osteoblasts and epithelial cells                        | - Type A gelatin                        | Freeze-gelation<br>Freeze-drying               | 20–125         | 85           | [15,16]   |
|  |   | - Collagen                              |  | 250–500        | -            |           |
|  |   | - CG<br>- Starch                        |  | 325            | -            |           |
| Cell infiltration                        | - Dermal fibroblasts<br>- Primary rat osteoblasts   | - Synthetic human elastin               | Electrospinning                                | 11             | 34.4         | [17,18]   |
|  |   | - PHP                                   | Phase separation                               | 100            | -            |           |
| Angiogenesis                             | Multilayer agent-based model simulation   | PEG                                     | Freeze-drying                                  | 160–270        | -            | [19]      |
| Bone tissue regeneration                 | Human osteosarcoma (MG63)   | chitosan/carboxymethyl cellulose        |  | 35–200         | 61–75        | [20]      |

Note: Bone marrow cells (BMC); adipose stromal cells (ASC); human mesenchymal stem cells (hMSC); polyethylene glycol (PEG); polyHIPE polymer (PHP); polycaprolactone (PCL); poly (lactic-co-glycolic acid) (PLGA); gelatin/chondroitin/hyaluronate (GCH); hyaluronic acid (HA); collagen-gelatin (CG).

## 2. Porous 3D Scaffolds

### 2.1. Fabrication of Porous 3D Scaffolds

To obtain a commercially and clinically viable tissue engineered construct, it should be cost effective and possible to scale-up from laboratory to batch production [21]. Porous structured materials can be obtained from the wet gel by effectively removing the solvent while maintaining the structure backbone without collapsing or breaking. Therefore, there are various techniques that enable the obtention of scaffolds for tissue regeneration in a predictable and reproducible manner using different biomaterials. Table 2 summarizes the advantages and disadvantages of 3D scaffold fabrication by various techniques, showing that it is very important to choose an appropriate method for 3D scaffold fabrication. A recent review by Barrios et al. has critically reviewed 3D porous material production from different nanomaterials [22]. Recently, supercritical CO<sub>2</sub> drying and freeze-drying have been widely used to produce scaffolds with high porosity, low density, and high specific surface [23–25]. Such porous materials are called aerogels, and their preparation involves the following three steps: Solution transition, which is preparing a colloidal solution through dispersion of polymer in the solvent. Secondly, sol–gel transition occurs by cross-linking the polymer solution to form a coherent network. Finally, gel–aerogel conversion induces air into the solvent wet-gel to form the micropores.

**Table 2.** Pros and cons of 3D scaffolds fabrication by various techniques.

| Fabrication Technique                      | Pros   | Cons  | References |
|--|--|---|------------|
| Solvent casting and particulate leaching   | Tunable pore size<br>Control facile process  | Limited pore interconnection<br>Not many solvent choices<br>Use of harsh chemicals  | [26]       |
| Phase separation                           | Desirable structure control  | Limited solvent choice<br>Not user friendly   | [27]       |
| Gas foaming                                | High level of pore interconnectivity   | Unsustainable processing<br>Low kinetic stability   | [28]       |
| Hydrogel microfabrication                  | Fine structure design<br>Tuneable mechanical properties  | Limited interconnectivity to obtain 3D structure<br>Limited material choices  | [29,30]    |
| Electrospinning (ES)                       | Ultra-Fine fiber size tenability<br>Wide range of material choices                                 | Prone to the ES environment<br>Limited fiber density control<br>Challenging repeated performance<br>Limited interconnectivity of fibers   | [31,32]    |
| Vacuum drying and microwave drying methods | Interconnected meso- and microporous structure   | Large pores and leading to collapse   | [33]       |
| 3D printing                                | Facile processing<br>Ultrafine structure control<br>Sustainable<br>Desirable mechanical properties | Limited material options<br>Inadequate printing resolution  | [34,35]    |
| Supercritical CO <sub>2</sub> drying       | High surface area<br>High pore volume<br>Prevent shrinkage or collapse of mesopores                | Use of organic solvents<br>Safety hazards due to its high-pressure operation<br>Relatively toxic drying process.<br>Energy and time consumption which increases the high overall cost process | [23,36]    |
| Freeze-drying                              | Sustainable<br>Non-toxic solvent used<br>Low temperature process<br>Inexpensive                    | Limited mechanical properties<br>Large pore size range  | [37,38]    |

Compared to other techniques, the distinct advantage of freeze-drying is more sustainable and cost effective. In addition, the freeze-drying process is particularly favorable for the development of valuable biomaterials that are heat sensitive. During freeze-drying, the solvent, which is typically water, goes directly from ice to vapor by the sublimation process at low temperature. It can be used to produce

3D scaffolds in the form of a sustainable aerogel from various applications, including biomedical applications. Therefore, this part of the review is mainly focused on freeze-dried aerogel preparation and factors influencing the aerogel formation.

Freeze-drying is also called “lyophilization”, where the dry structures (aerogels) bypass the phase boundaries through a three phase steps [39]. In order to prepare aerogels through freeze-drying, an aqueous precursor is required to form a “hydrogel” initially. Then hydrogels are frozen to form ice crystals prior to being sublimed in vacuum to obtain aerogels. Furthermore, the freezing temperature and direction (unidirectional freezing) can alter the sizes of the pores, producing honeycomb or lamellar morphologies [37,40]. By using the unidirectional freezing technique, the suspension (gel) is aligned with the freezing direction since the gel is in contact with the freezing medium directly, and the ice crystals grow perpendicular to the freezing medium [40]. Freeze-drying can offer 3D aerogel scaffolds with porosity of up to 99%, which is greatly beneficial for in vivo implant tests because it provides sufficient capacity for vascularization and nutrition transformation. The first patent for freeze-drying applications of biological material was recorded in 1927 for blood serum regeneration [41,42]. However, the scaffolds obtained by this technique can be challenged due to inadequate mechanical strength of the scaffolds because of the highly porous structure. Obtaining a balance between mechanical properties and porous architecture in scaffolds for cell infiltration is a key challenge for an optimum porous scaffold by the freeze-drying process.

## 2.2. Parameters Influencing the Freeze-Dried Porous 3D Scaffolds

To obtain a desirable property for scaffold through freeze-drying technique, the structure must offer homogenous distribution of pores. Instrumental and hydrogel properties are two main factors which can influence the final properties of the freeze-dried aerogels. The instrument-related concerns include the freezing temperature, drying temperature, chamber pressure, and type of mold used. The latter involves the concentration of solid content, viscosity of gels, and type of polymers. The cross-linking (physical or chemical or radiation) of freeze-drying hydrogels can also play an important role in determining the resultant aerogel properties [43]. Physical cross-linking of gels is due to the van der Waals forces, hydrogen bonds, hydrophobic or electronic associations, and chain entanglements. On the other hand, chemical cross-linking of hydrogels is realized by the addition of chemicals.

The rate of freezing is the most important factor in terms of the instrumental parameters. By altering and tuning the instrumental parameters, the morphology and size of the ice crystals, which control the pore sizes and porosities of aerogels, can be changed. Vansanthan et al. observed the effect of freezing temperature on the pore size and porosity of the scaffolds, where reducing the freezing temperature from  $-4$  to  $-20$  °C resulted in a reduction in pore size [44]. This study revealed that the annealing process can improve the properties of the scaffold, but it is not as effective as changing the freezing temperatures. The annealing process can occur during the freezing step wherein the frozen formulation is maintained above the ultimate freezing temperature for a specific time [45]. The preferred temperature for this process needs to be maintained between the melting temperature of ice and the glass transition temperature. Moreover, using a more rapid, higher rate of immersion through liquid nitrogen, a denser structure can be expected. This is more valid when a higher immersion rate leads to faster freezing of the composition and results in a heterogeneous structure [46]. Overall, depending on the subject tissue that needs to be reconstructed, it is possible to form a dense aligned 3D scaffold with small pore size by employing a fast freezing rate, or to form a tube-shaped 3D scaffold with higher porosity using a slower freezing rate (Figure 1) [44]. It is worth mentioning that the vertical cross-section of the 3D scaffold with a tube shape offers a different pore orientation compared to those with the horizontal cross-section.

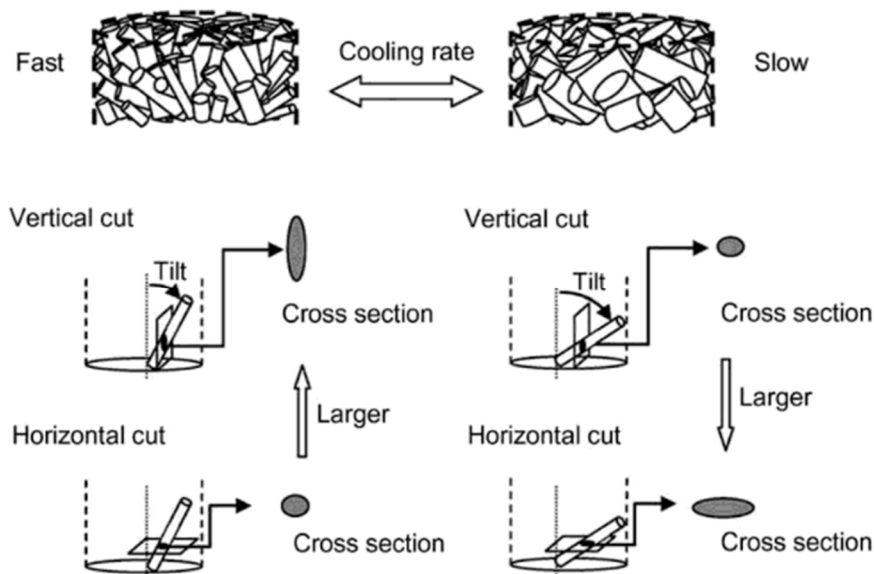


**Figure 1.** Schematic view of vertical and horizontal cross-sections of samples obtained through fast and slow freezing temperature. (Reprinted with permission from Chemical Engineering Research and Design, Vol. 89, Huihua Liu, Kyuya Nakagawa, Deeptangshu Chaudhary, Yusuke Asakuma, Moses O. Tadé. Freeze-dried macroporous foam prepared from chitosan/xanthan gum/montmorillonite nanocomposites 2356–2364, Copyright 2011, Elsevier) [37].

In order to obtain more aligned pores within the scaffolds, researchers utilized molds as an influencing factor to produce uniaxial thermal gradient. To obtain a preferably high thermal gradient, it has been suggested to insulate tube walls in such a way that the heat could travel only through the metal plate located at the bottom of the mold. The thermal conductivity of the mold is of great importance, as the temperature gradient established from the plate to the hydrogel controls the formation of ice crystals from the nuclei formed during the primary freezing [47]. The geometry and composition of the mold control the temperature gradient inside the sample. High thermal conductive aluminum has been highly recommended for the process, where anisotropic growth of ice crystals is obtained, resulting in the formation of lamellae in the direction of the temperature gradient (bottom towards the top). This mechanism is usually divided into three stages: the solution cooling phase, phase separation and the frozen solution cooling stage. During the first stage, heat conduction is the dominant heat transfer mechanism. In phase separation, the heat transfer via conduction followed by latent heat (heat required to vaporize the frozen water) release during phase change takes place. Ultimately, primary nucleation occurs only on regions in contact with the cold source, where release of latent heat caused by formation of the first nuclei prevents the nucleation of other nuclei in the other parts of the mold [47]. A study by Asuncion et al. showed that aerogel fabricated with silk fibroin–gelatin suspension using an aluminum mould has a better aligned structure than those made on a plastic mold, because the plastic mold offers 1600 times less heat conductivity than the aluminum mould [48]. The formation of aligned ice crystal structure is mainly due to the nucleation and unidirectional temperature gradients caused by the establishment of the aligned lamellar ice crystals, with peculiar anisotropic growth in the solidification direction [40]. The initial fast heat transfer from the substrate to the hydrogel can cause formation of a smaller ice crystal, and as the initial burst decreases, larger crystals are formed towards the middle of the sample [49].

### 3. Natural Polymer-Based Scaffolds

The use of appropriate materials for scaffold preparation is important because the scaffold fabrication process and applications are dependent on the type of biomaterials used. A biomaterial is defined as a material which will influence the biological systems to be evaluated, treated, augmented,

or will replace any tissue, organ, or function of the body [50]. In this context, there are various inorganic and organic materials that have been used as tissue engineering materials. As previously mentioned, among the biomaterials, natural polymers can offer various advantages over inorganic biomaterials and synthetic polymers, such as outstanding biocompatibility and biodegradability, resulting in excellent cell attachment and proliferation. The naturally derived polymers have shown great potential for tissue engineering applications [51]. In addition, most of the proteins (e.g., gelatin, collagen, soy, egg white, silk fibroin, etc.) and polysaccharides (e.g., cellulose, chitosan, alginate, starch, pectin, agar, etc.) can form a loose viscoelastic gel in aqueous solution (hydrogel) through non-covalent interaction/cross-linking, because they possess high density of surface functional groups, e.g., amino groups on chitosan or carboxyl groups on pectin or alginate, opening up new applications and providing convenient anchoring points for added functionality [52,53]. Such hydrogels can absorb water up to thousand-folds of their dry weight and create a gel-like environment, mimicking stem cell niche [54]. Cellulose- and chitin-based hydrogel preparation and their applications have been critically reviewed by Shen et al. [55]. The physical cross-linking can occur through hydrogen bonding, ionic interactions or physical entanglements. Hydrogen bonding cross-links are typical of protein and nucleic acid aerogels, but they are also common for polysaccharide aerogels, e.g., pectin, cellulose, chitosan and alginates either through intermolecular hydrogen bonds or through hydrogen bonds with cross-linkers [52]. Radiation cross-linking and ionic cross-linking can be used to increase the stability of cellulose, starch, chitosan and alginate gels [52]. The detailed chemistry of the proteins and polysaccharides have been reported by Zhao et al. [52].

Proteins (e.g., collagen) are the most frequently used natural polymers for scaffold fabrication due to their inherently similar composition to natural ECM, excellent biocompatibility, hydrophilicity biodegradability and cost effectiveness [56,57]. The importance of resembling ECM role in tissue culture is crucial, therefore, collagen as the main component of ECM has received extensive attention as a natural polymer source for various clinical applications [58,59]. However, there are still potential drawbacks for using collagen, such as antigenic and immunogenic responses for *in vivo* applications [60]. Amongst the products of partial hydrolysis of collagen, gelatin has proven to provoke lower immunogenicity *in vivo*, which promotes its use as a biopolymer in scaffold fabrications [60]. There are limitations with the use of gelatin and natural polymers in general for biomedical applications. The potential impurities in different sources of extraction can cause unexpected immune rejection *in vivo* [38,61]. Moreover, polymers such as gelatin show poor mechanical properties, which results in difficult substrate handling and serious deformation during both *in vitro* and *in vivo* clinical applications [62]. Therefore, proteins should be incorporated with other physiochemically robust polymers such as cellulose to maintain the structure for biomedical applications [63].

The other promising type of natural polymers used for scaffold fabrication is polysaccharides. Polysaccharides are carbohydrate polymers, which are composed of a number of mono-saccharide units connected by glycosidic linkages [33]. The polysaccharides are mainly extracted from plants and some are from animal sources. Amongst them, starch is shown to be promising for fabricating scaffolds since it is renewable, easily available at low cost, biocompatible, and highly biodegradable [64]. Starch can be plasticized with glycerol, water, and sorbitol used for scaffold template. Furthermore, it offers similarities to ECM, low risk of immunological rejection, as well as distinct tuneable structural forms. The main disadvantageous of starch is its low mechanical stability and water sensitive, as per any other natural source polymers [40]. However, this drawback can be compensated by reinforcing starch with another biopolymer to form a robust biocompatible scaffold. Similarly, alginate can also be combined with other natural polymers to achieve desired performance for biomedical applications [65].

Recently, the use of renewable cellulose as an replacement for micro-sized reinforcement in composite materials has attracted much attention [66]. Cellulose is a homopolysaccharide composed of  $\beta$ -1, 4-D-glucopyranose units, and has a strong tendency to create intramolecular hydrogen bond networks that results in interchain cohesion and formation of crystalline regions [67]. Such polymers hardly exert any toxicity on cells and are highly biocompatible, but they provide limited support for

cell adhesion and proliferation. Cellulose made of renewable sources is considered a promising natural biomaterial for biological applications due to its high water uptake capacity, flexibility, high porosity and excellent mechanical properties [63,68]. Cellulose has been used to produce suspension, hydrogels and aerogels, film or tablets for drug delivery applications. Recently, porous 3D-structured scaffolds prepared from the cellulose hydrogels via solvent removal have attracted great interests for tissue engineering applications [69]. Based on the cellulose production/preparation methods, cellulose can be carboxymethyl cellulose, microfibrillated cellulose, cellulose nanocrystals, bacterial cellulose, cellulose nanowhiskers, and cellulose nanofibrils. Carboxymethyl cellulose (CMC) is obtained by carboxylation of cellulose, which is non-toxic, biodegradable, biocompatible and soluble in water. Therefore, CMC can be used in dermal tissue engineering, pulp cell regeneration, protein delivery and prevention of post-surgical adhesions [70,71].

Microfibrillated cellulose (MFC) is long cellulose microfibrils with diameters from 20 to 60 nm and is produced by mechanical disintegration of cellulosic materials. It contains both a crystalline and amorphous structure, and has a very good ability to form a stable network, which could be ideal for the production of hydrogels [71,72].

Cellulose nanocrystals (CNC) are mainly produced by acid hydrolysis from cellulose fibers, where amorphous parts of the raw materials are removed. They possess a desirable modulus of elasticity (150 GPa), and low thermal expansion coefficient ( $\sim 10^{-7} \text{ K}^{-1}$ ) due to their rigid rod-like nanocrystal (dimensions of 4–24 nm  $\varnothing$ , and hundreds of nanometer in length) structure [73]. There have been several studies on the cytotoxicity of CNC using different cell types, and no toxic effect was observed [74,75].

Cellulose nanowhiskers (CNW) are suspensions of fibrous structures with diameters similar to nanofibrils, but shorter in length produced via sulfuric acid hydrolysis of native cellulose [7,76]. CNW have needle-like or rod-like morphology with a higher crystallinity index compared to cellulose nanofibers. Several studies have demonstrated that colloidal suspensions of CNW may be slightly cytotoxic, but may also cross the plasma membrane of cells, pointing to applications in targeted drug delivery and bioimaging [76]. CNW could provide nanoscale structural cues to direct cells in tissue engineering applications.

Bacterial nanocellulose (BNC) is obtained by cultivation of different bacterial strains (e.g., *acetobacterxylinum*) in culture media [77]. Bacterial cellulose has fascinating properties, such as high crystallinity (>85%), high degree of polymerization ( $\sim 10,000$ ), high purity, excellent mechanical properties (Young's modulus of 15 GPa), high water uptake at dry state and nano-structured dimensions [78]. BNC gels can be easily molded into desired shapes and sizes, hence, BNC is greatly favorable in the food industry as a dietary fiber and in biomedical engineering as skin substitutes and artificial blood vessels [79,80]. In vitro and in vivo proof-of-principle studies of BNC have been carried out for bone, cartilage, and nerve tissue engineering [76,81,82]. A study by Torgbo and Sukyai stated that BNC is an attractive option for bone tissue implants due to its excellent mechanical properties and biocompatibility [83]. However, it was observed that the degradation of BNC is not fast enough after implantation, which makes it not an ideal option for osseointegration. The degradability of BNC needs to be altered through chemical, enzymatic, and genetic engineering methods to make it more suitable for various tissue engineering applications.

Cellulose nanofibers (CNF) are typically prepared by grinding, homogenization and applying high shear forces through defibrillation of cellulose fibers. Different surface chemistries can be used to produce CNF for various applications. For instance, 2,2,6,6-tetramethylpiperidine-1-oxyl radical (TEMPO)-mediated oxidation introduces functional groups by providing aldehyde and carboxylic acid groups in the C6 position, mild carboxymethylation gives carboxymethyl groups, and periodate oxidation introduces aldehyde groups in position C2 and C3 of cellulose [84,85]. It was also reported that the surface of CNF can be oxidized into dialdehyde by sodium periodate, which offers active sites for introducing active molecules [86]. The other characteristic that makes CNF an ideal biopolymer for scaffold fabrication is its excellent mechanical properties [53]. It was reported that the CNF extracted

from wood pulp has a Young's modulus of 30–40 GPa [87]. The other factor that influences the stiffness of the CNF aerogels matrix is the charge density of the fibrils. The TEMPO modified CNF (T-CNF) aerogels usually have two different charge densities of  $1.14 \pm 0.07$  mmol/g (considered low charge) and  $1.71 \pm 0.04$  mmol/g (considered high charge), and their effects on cell proliferation have been studied, with low charge T-CNF showing better cell proliferation and attachment [67]. CNF with adequate stiffness can significantly influence human mesenchymal stem cell responses, and it enables the cells to try to push and pull within their microenvironment [88].

CNF can be used to form suspensions depending on the charge density, fibrillation degree and fibril length if the solid content is about 0.5 wt.% [89]. The fibril entanglement, ionic interactions and hydrogen bonds can hold such fibril dispersions [90]. The elasticity of the gels can be improved by increasing the solid content in the composition, and the modulus follows a power-law relation with solid content of the CNF dispersions [91]. The extensive hydrogen bond within CNF results in high thermal stability as well as Young's modulus [92]. If there is no covalent bonding between fibrils in the gels, then it is mechanically weak, and it can easily be destroyed once their chemical characteristics are altered or they are subjected to a mechanical force. Such stability can be increased by covalent cross-linking, where another biopolymer is combined in the matrix to form permanent composite gels prior to producing porous 3D aerogel scaffolds.

### 3.1. Cellulose Porous 3D Aerogel Scaffolds Preparation by Freeze-Drying

Cellulose-based porous 3D scaffolds are prepared for tissue engineering applications because of their biocompatibility, biodegradability, and good mechanical properties. For instance, nanocellulose 3D aerogel scaffolds with high porosity and surface showed effective cell growth and proliferation [33]. A study by Krontiras et al. fabricated a freeze-dried 3D cross-linked homogenized BNC scaffold to obtain a porous structure [93]. This study cultured mesenchymal stem cells of the line C3H10T1/2 from mouse embryos incubated in adipogenic medium. The 3D BNC scaffolds showed more cells with improved adipogenic cell differentiation compared to 2D BNC scaffolds, as well as the potential for reconstructive surgery after trauma or congenital defects. Different cross-linkers, i.e., glucose, vanillin and citric acid, were used to improve the bacterial cellulose scaffolds for tissue engineering applications [80]. In vitro studies of these scaffolds showed non-cytotoxic and no inflammatory response in macrophages.

CNC-based 3D aerogels have also been produced by direct ink writing followed by freeze-drying [94]. Figure 2 shows that the complex and customizable inner pore architectures can be obtained without structural collapse or shrinkage during aerogel production for potential tissue scaffold templates. Similar to CNC, direct ink-writing 3D-printed CNF hydrogels were explored to produce aerogels by direct drying as well as freeze-drying [95]. The freeze-dried method exhibited a highly porous structure without much shrinkage, whereas the air-dried aerogel collapsed in the z-direction. These freeze-dried CNC aerogels could be potential candidates for tissue regeneration applications. A study compared the fibroblast cell proliferation behavior of TEMPO-oxidized CNF (T-CNF) and carboxymethylated cellulose (CMC) with respect to their surface chemistries [90]. No toxicity was observed for both scaffolds. The 3D cell culture test of fibroblasts on CMC showed poor morphology and spreading of the cells. On the other hand, T-CNF aerogels showed healthy morphology and fine spreading of the cells. A significant decrease in cell attachment and proliferation was reported on CMC as compared to those on T-CNF [90]; it is attributed to the surface chemistries of scaffolds.

Cross-linked CNF aerogel microsphere scaffolds were produced by the spray-freeze-drying method for cell culture studies [96]. The CNF aerogel microspheres showed porosity from a few nanometers to micrometers throughout the sample (Figure 3). When the CNF concentration or cross-linker concentration was increased, denser aerogel microspheres with smaller pore size were obtained. Figure 3f shows that the sizes of CNF aerogel microspheres are in the range of a few tens to hundreds of micrometers. It was observed that the CNF aerogel microspheres are nontoxic and biocompatible. Therefore, the interconnected high porous nanofibrous structure could facilitate cell attachment,

penetration, differentiation, and proliferation and allow proper transfer of nutrient/oxygen and metabolic waste [96].

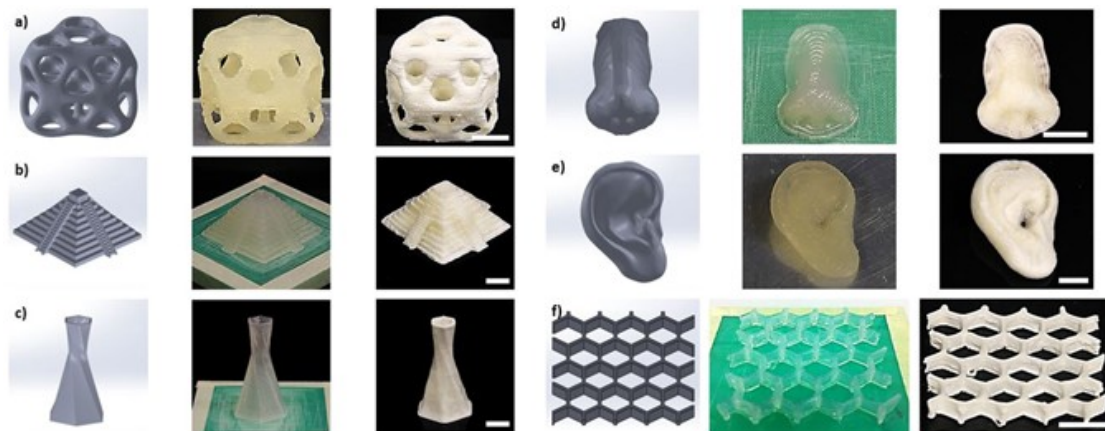


**Figure 2.** Direct ink write (DIW) 3D-printed (a) octet cube, (b) pyramid, (c) hexagonally twisting vase, (d) nose model, (e) ear model, and (f) honeycomb from 20 wt.% cellulose nanocrystal (CNC) gel and 500  $\mu\text{m}$  nozzle tip. The first column is a Computer-Aided Design (CAD) model, the second column is DIW 3D-printed gel structures, and the third column is the resultant structures after freeze-drying. Displayed scale bars are 1 cm. (Adapted from Scientific Reports, Vol. 5, Vincent Chi-Fung Li, Conner K. Dunn, Zhe Zhang, Yulin Deng and H. Jerry Qi, Direct Ink Write (DIW) 3D Printed Cellulose Nanocrystal Aerogel Structures, 8018, Springer Nature, 2017) [94].

One of the main advantages of using CNF is the appearance of the OH groups in different chemical modifications, which can promote cell attachment and proliferation [67]. The surface wettability is also within the optimum range (contact angle of  $47^\circ$  for T-CNF), which has been proven to promote cell adhesion and proliferation during *in vitro* experiments [97]. A study by Bhattacharya et al. reported that the nutrient diffusion rate of an aerogel (1.7 wt.% CNF) is comparable to those of proteins existing on native ECM [98]. This suggests that CNF-based structures offer adequate diffusivity of nutrients for the cells in 3D scaffolds. Vartiainen et al. assessed the viability of an cytokine behavior of a mechanically derived CNF suspension with different concentrations, where they observed no cytotoxic effects on cells after 6 and 24 h in culture media [99]. Another study investigated the cytotoxicity of T-CNF and unmodified CNF, where no toxicity was observed on the cell membrane, cell mitochondrial activity and DNA proliferation [100]. Further investigation showed that by cross-linking the samples using polyethyleneimine, cell viability was significantly reduced. Similarly, freeze-dried CNF shows fibroblast cells attachment on its surface, which confirms no cytotoxicity. On the other hand, an aerogel made of T-CNF cross-linked with polydopamine and tetracycline was active against *Staphylococcus Aureus*, resulting in enhanced healing of the skin inserted on rats *in vivo* [101]. Birch wood pulp-sourced CNF modified with TEMPO-mediated oxidation exhibited a lower pro-inflammatory response compared to unmodified CNF using human dermal fibroblast *in vivo* [102]. CNF produced from sawdust was proven to cause inflammation in mice, determined by increasing the leukocytes and eosinophils on mice lungs [103]. This result was also consistent with another study by Shvedova et al., where mice exposed *in vivo* to respirable untreated sawdust-derived CNF resulted in pulmonary inflammation and damage, increased collagen level and transformation of the growth factor in mouse lungs [104]. Therefore, cellulose has been blended with different bioactive natural polymers to enhance the biocompatibility while maintaining the biodegradability, mechanical properties and structure [105].

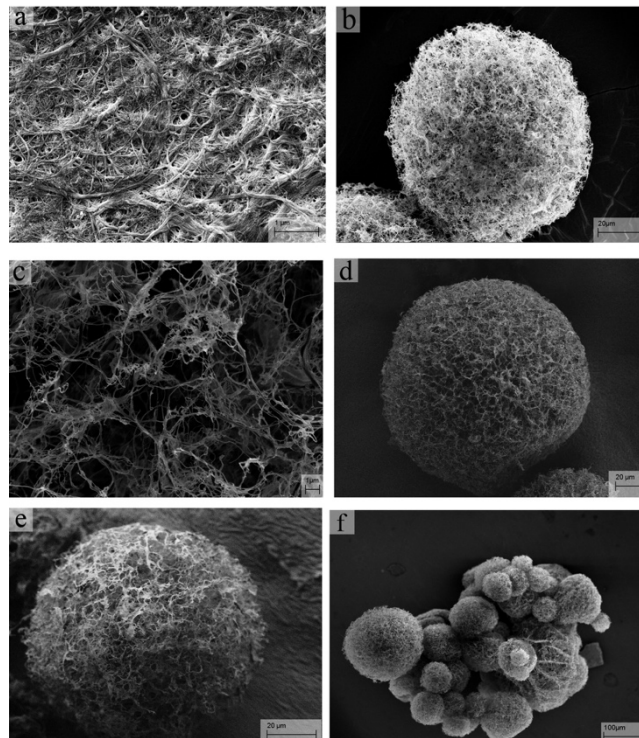


**Figure 3.** SEM of the aerogel microspheres with a different cellulose nanofibril concentrations or cross-linker ratios (cellulose nanofibrils to cross-linker,  $w/w$ ): (a) image of native nanofibrils (scale bar 1  $\mu\text{m}$ ); (b) image of aerogel microspheres with a nanofibril concentration of 1.5% and a cross-linker ratio of 10:1 (scale bar 20  $\mu\text{m}$ ); (c) image of aerogel microspheres with a nanofibril concentration of 0.6% and a cross-linker ratio of 10:1 at higher magnification (scale bar 1  $\mu\text{m}$ ); (d) image of aerogel microspheres with a nanofibril concentration of 2.0% and a cross-linker ratio of 10:1 at higher magnification (scale bar 20  $\mu\text{m}$ ); (e) image of aerogel microspheres with a nanofibril concentration of 0.6% and a cross-linker ratio of 10:2 (scale bar 20  $\mu\text{m}$ ); (f) low-magnification image shows multiple cellulose nanofibril aerogel microspheres (scale bar 100  $\mu\text{m}$ ). (Reprinted with permission from Biomacromolecules, Vol. 15, Hongli Cai, Sudhir Sharma, Wenying Liu, Wei Mu, Wei Liu, Xiaodan Zhang, and Yulin Deng. Aerogel Microspheres from Natural Cellulose Nanofibrils and Their Application as Cell Culture Scaffold, 2540–2547, Copyright 2014, Journal of American Chemical society (ACS)) [96].

### 3.2. Cellulose Composite-Based 3D Porous Aerogels

Composites have been studied extensively for scaffold fabrication, and the main challenge is to obtain optimal matrices with adequate mechanical properties that act as cell carriers for tissue regrowth and regeneration. To be useful for scaffolds for tissue engineering applications, the cytotoxicity and immunogenicity of cellulose need to be tuned by the addition of another biocompatible composition. The scaffolds can be strengthened by various techniques to obtain a more robust 3D cellulose structure. For example, biologically active molecules such as polysaccharides, proteins, glycosides, cytokines growth factors and nanoparticles can be combined with cellulose to form cellulose-based scaffolds with better functionality. Naseri et al. studied the effect of chitosan enclosure into CNF to produce freeze-dried porous 3D composite scaffolds for cartilage tissue regeneration [106]. It was also observed that the mechanical properties of the composite were reduced by inclusion of the second component. However, a minimum concentration of the CNF matrix phase was found to be necessary to bind the fibers together, which ensures stability of the scaffold and promotes cell interaction with the microenvironment. Three-dimensional porous architecture was prepared with calcium chloride ( $\text{CaCl}_2$ ) cross-linked CMC/pectin with 0.1% MFC (C(0.1%)) for tissue engineering scaffold [71]. Figure 4 shows the micro-CT images (side- and cross-section view) of the CMC/pectin/MFC scaffold, indicating that the pore size is in the range of 15–280 microns (Figure 4d) with 88% porosity (Figure 4c). These scaffolds

showed improved mechanical properties because of the formation of interpolymer complexes with secondary bonds. The resulting scaffolds showed in vitro degradation with the highest cell viability on the NIH3T3 fibroblast cell line [71].

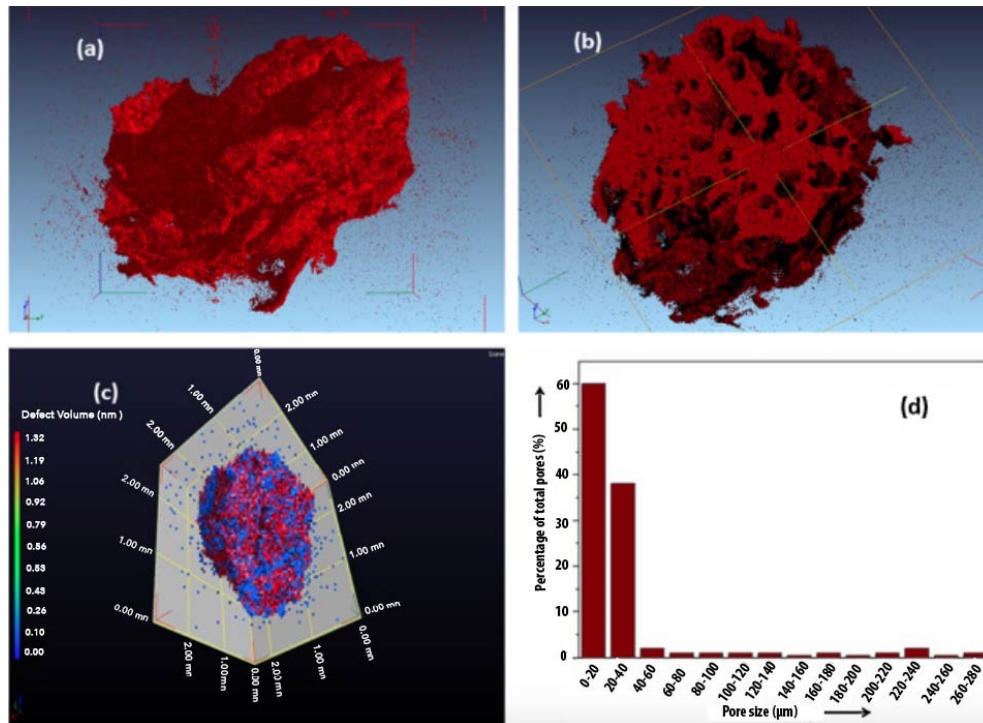


**Figure 4.** Micro-CT images: (a) side view, (b) cross-sectional view of (c) defect volume analysis for estimation of porosity. (d) Pore size distribution of C (0.1%). (Reprinted with permission from Carbohydrate Polymers, Vol. 98, Neethu Ninan, Muthunarayanan, In-Kyu Park, Anne Elain, Sabu Thomas, Yves Grohens. Pectin/carboxymethyl cellulose/microfibrillated cellulose composite scaffolds for tissue engineering, 877–885, Copyright 2013, Elsevier) [71].

Starch, collagen, and gelatin are other interesting bioderived polymers that can be combined with cellulose to form composite scaffolds. There have been recent studies to evaluate the effects of starch, collagen, and gelatin incorporated with CNF for wound healing and drug delivery applications [107]. Incorporated gelatin and starch 3D constructs can potentially swell a large amount of water (typically up to 100 times its dry mass), and provide a suitable in vitro culture platform to investigate further the behavior of ECM environment for tissue regeneration [62]. Collagen was incorporated with a sodium periodate-oxidized cellulose nanofiber matrix to form cross-linking through the bonds of Schiff base [86]. As a result, composite aerogels were formed by bonding collagen along dialdehyde nanofibers. The CNF/collagen composite aerogels exhibited 90–95% porosity, up to 4000% water absorption, good biocompatibility and a high level of cell activity and proliferation, which may be suitable for tissue engineering scaffolds [86]. Carlström et al. prepared aerogel from cross-linked gelatin–CNF hydrogel (dehydrothermal treatment cross-linked (Gel-CNF1) and hexamethylenediamine cross-linked (Gel-CNF 2) CNF by freeze-drying for tissue engineering scaffold application [108]. The morphology, cell attachment and cell viability of CNF and the gelatin–CNF composite are presented in Figure 5. These composite aerogels showed porosity higher than 70% with a pore size of 8–150 microns and a surface area of higher than 1274 mm<sup>2</sup>. The produced scaffolds supported cell attachment, spreading, and osteogenic differentiation. After 1 day of cell culture, CNF scaffolds showed more cells attached onto them compared to the gelatin–CNF groups (Figure 5F). This phenomenon was attributed to a highly hydrophilic and anionic-charged CNF surface, which results in superior protein adsorption and facilitates cell attachment. Live/dead assessment revealed high cell viability (green) with few dead

cells (red) after 1 and 7 days (Figure 5C,D). Quantification of cell viability by the release of lactate dehydrogenase (LDH) (Figure 5E), revealed that LDH levels in the test groups were comparable with the known non-cytotoxic material in the control group. The results suggest that cross-linked gelatin–CNF composites are cytocompatible and potential biomaterials for tissue engineering application [108]. The same research group studied gelatin–CNF aerogels with a number of chemical cross-linkers for tissue regeneration application [38]. The designed 3D structure scaffolds underline interconnected porosity achieved by the freeze-drying process, improved mechanical properties and chemical stability that are tailored by CNF addition and different cross-linking approaches. In vitro evaluations reveal the preservation of the biocompatibility of gelatin and its good interaction with cells by promoting cell colonization and proliferation. The results support the addition of cellulose nanofibrils to improve the mechanical behavior of 3D porous structures suitable as scaffolding for tissue regeneration [38].

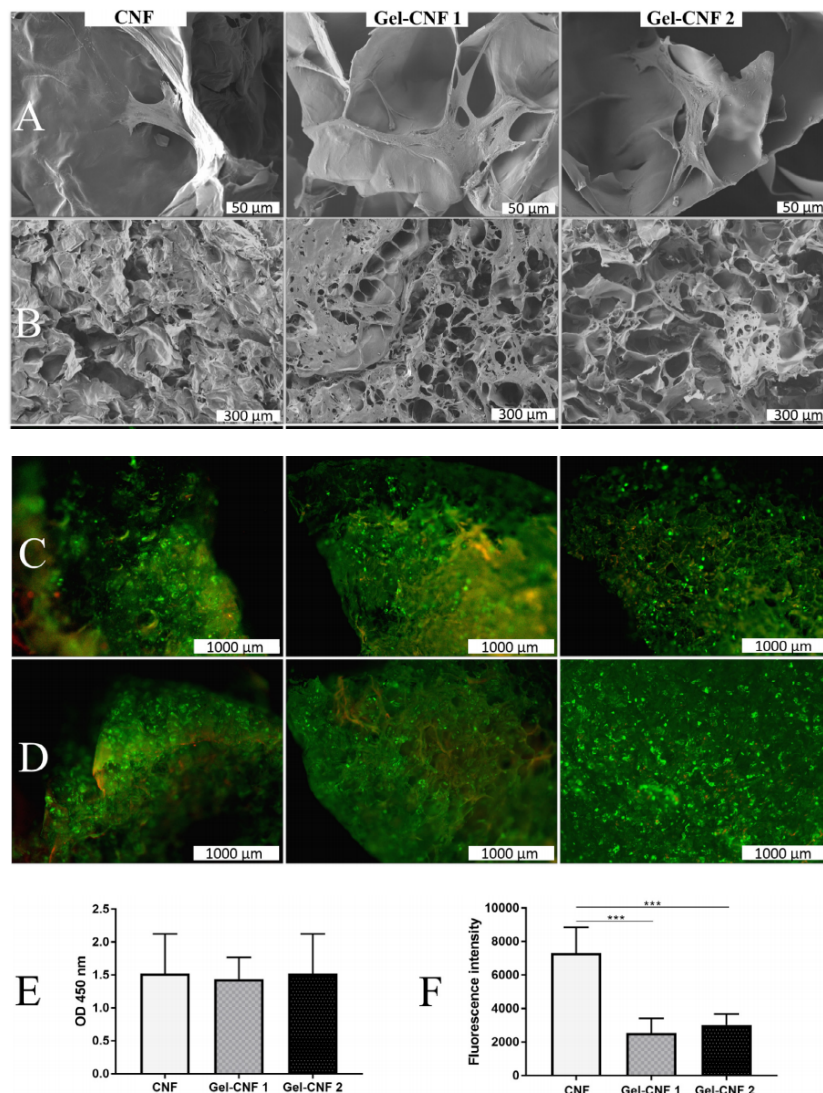


**Figure 5.** Cell–scaffold interactions in terms of cell attachment, morphology and viability. Attachment of hBMSCs by SEM after 1 (A) and 7 days (B). Live/dead assay after 1 (C) and 7 days (D). Live cells are stained green, and dead cells are stained red. (E) Cytotoxicity assessment by lactate dehydrogenase (LDH) assay after 1 day. (F) PicoGreen assay quantifying cell attachment after 1 day. ( $p < 0.001$ ) (Reprinted with permission from Materials Letters, Vol. 264, Ingeborg Elisabeth Carlström, Ahmad Rashad, Elisabetta Campodoni, Monica Sandri, Kristin Syverud, Anne Isine Bolstad, Kamal Mustafa. Cross-linked gelatin-nanocellulose scaffolds for bone tissue engineering, 127326, Copyright 2020, Elsevier) [108].

Liu et al. investigated the effects of hemicellulose (xylan, xyloglucan and galactoglucomannan) on CNF aerogels with different ratios. Most of the aerogels produced from CNF-hemicellulose were highly charged, which had a negative influence on cell growth and viability [102]. Another possible reason for limited cell proliferations can be associated with the observed low Young's modulus (10–50 kPa). Even though CNF offer specific characteristics (high surface area and modulus) that are suitable to be used as a reference matrix for the composites, there are only limited natural polymers blended with cellulose to produce composites. This is mainly due to the restricted hydrophilicity of the CNF, as well as the irreversible aggregates that are formed once dried [99]. Moreover, obtaining a uniform dispersion of the CNF fibrils is a hurdle because of the high surface energy and the appearance of hydroxyl groups on the surface of the CNF. Therefore, there are many studies that investigated the CNF-incorporated synthetic water-soluble polymers by freeze-drying for tissue engineering applications [109].

### 3.3. Cellulose Composite-Based 3D Porous Aerogel Scaffolds with Antibacterial Agents

Cellulose is inherently considered as a potential biomaterial for tissue engineering application, particularly for wound healing, due to its excellent physiochemical, mechanical and biological properties; however, it does not possess any antibacterial properties if used on its own [7,62]. If cellulose-based scaffolds are used for wound healing applications, offering antimicrobial properties is essential. Moreover, skin injuries provide a gateway for pathogenic bacterial (such as *Staphylococcus aureus*) that can either exist in tissue microbiota or acquired from the environment, which results in tissue remodeling impairments. There are several pathogens in skin infections such as bacteria genus (*Acinetobacter*, *Enterococcus*, *Escherichia*, *Klebsiella*, *Pseudomonas*, *Staphylococcus*, and *Streptococcus*) [51]. Therefore, it is essential to incorporate antibacterial agents. Silver nanoparticles are metal-based agents that can be incorporated in cellulose since they are an active agent against *Pseudomonas aeruginosa*, *Escherichia coli*, and *Staphylococcus* [110]. For instance, silver nanoparticle-incorporated BNC-based aerogels showed increased antibacterial activity against *Escherichia coli* and *Staphylococcus aureus* [111]. It was observed that the cell adhesion onto the BNC surface was declined after incorporation of silver nanoparticles because of the reduced hydrophilicity nature of resultant BNC-based aerogels. Another study investigated curcumin as a stimulating antimicrobial compound for the composite. Curcumin is obtained from a natural source polyphenolic isolated from *Curcuma longa* and is a newly arrived compound in the tissue engineering field. The application of curcumin is limited to date due to its low water solubility, resulting in low bioavailability. Moreover, curcumin is almost insoluble in polar solvent and it tends to be unstable in alkaline pH (mainly degrades in ferulic acid and vanillin) [112]. However, curcumin can be incorporated with chemically modified CNF for wound dressing application. It offers excellent antimicrobial, anti-cancer and anti-inflammatory response to the cells, making it an interesting additive for tissue engineering application [113]. Such material can be coated onto the backbone of the nanocellulose composites, and the resultant scaffold can be utilized as soft tissue fillers, subsequently promoting wound healing [114]. The curcumin degradation was experimented by thermal decomposition at temperatures of 180 and 300 °C. The results obtained by incorporating curcumin into bacterial cellulose degraded at 180 °C suggested reduction of growing colonies of *Staphylococcus epidermis*. Further in vitro tests conducted on dermal fibroblasts revealed a significant cytotoxicity effect of curcumin degraded at 180 °C, whereas curcumin degraded at 300 °C enhanced and supported cell adhesion, growth and spreading (Figure 6). It is important to note that the antimicrobial activity and cytotoxicity of the curcumin depend on its concentration or its degradation products. Overall, balancing antibacterial properties with sufficient biocompatibility need to be considered when making composite scaffolds for tissue engineering applications. Biocompatible and biodegradable polysaccharides such as chitosan can be blended with cellulose to produce effective antibacterial scaffolds for biomedical applications [115,116]. Recently, a study investigated the antibacterial, mechanical, biocompatibility and in vitro coagulation ability of a modified CNF/chitosan aerogel for biomedical applications [117]. It was found that the aerogel has compressive strength of up to

75.4 kPa with high water absorption capacity, rapid shape recovery and good antibacterial activity. This antibacterial aerogel showed good adhesion as well as a good biocompatibility.

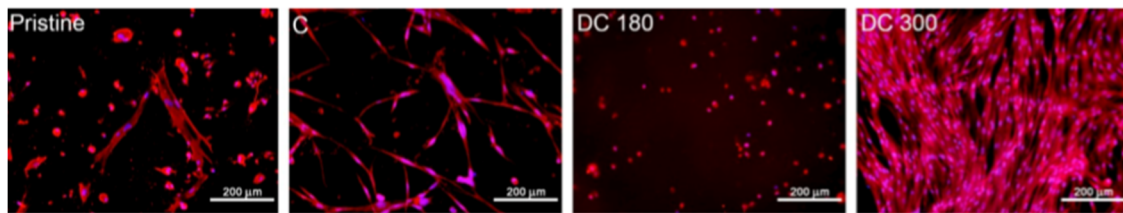


**Figure 6.** Digital images of human dermal fibroblasts cultured on bacterial cellulose after seven days of cell seeding in pristine incorporated with curcumin (C) degraded at 180 °C (DC 180 °C), and 300 °C (DC 300 °C). The cells shown were stained with Texas Red C2-Maleimide (red fluorescence, cell membrane and cytoplasm) and Hoechst #33258 (blue fluorescence, cell nuclei). (Adapted from *Nanomaterials*, Vol. 9, Lucie Bacakova, Julia Pajorova, Marketa Bacakova, Anne Skogberg, Pasi Kallio, Katerina Kolarova and Vaclav Svorcik. Versatile Application of Nanocellulose: From Industry to Skin Tissue Engineering and Wound Healing, 164, 2019) [7].

#### 4. Conclusions

The complexity of tissue engineering lies within the interplay of living cells, scaffolds, nutrients and signaling factors. Good scaffolds are able to aid cells and provide guidance to form tissue. In this respect, an appropriate design is of the ultimate priority for successful fabrication of scaffolds. Cellulose is a natural polymer which provides good properties that could make them a promising biomaterial for the fabrication of scaffolds for tissue engineering. Cellulose mimics the collagen proteins in the native ECM, and it offers robustness due to the fact that it is highly crystalline with tuneable matrix elasticity via adjustment of the cellulose content. Cellulose can form hydrogels at low solid concentration, and its surface chemistry can be altered due to the high number of OH groups. Cellulose-based hydrogels can be used to produce porous 3D scaffolds by sustainable and inexpensive freeze-drying techniques for tissue engineering applications. However, the degradation of cellulose in the human body remains a concern as the body does not have the chemical or enzymatic activities suitable for cleaving glycosidic linkage between the monomers. To overcome this issue, an appropriate bioactive material (e.g., proteins, carbohydrates, etc.) should be incorporated with cellulose to tune and alter the enzymatic degradation.

Tissue engineering is known to be a slowly evolving process as it deals with living organs in various levels. There are numerous factors to be investigated thoroughly in developing a tissue engineering construct, such as the design of the scaffolds and its functionality, interaction of cells with the scaffolds' microenvironment, survival of the cells, and the targeted application (bone, heart, liver, skin etc.), where each requires cells of certain criteria to mimic natural human functions. Further advancement in preparing 3D scaffolds needs to be explored to fabricate a macro-sized construct with long-term safety. The improvement of scaffolds with interconnected pores is vital, as they replicate the functionality of ECM, and employing advanced 3D printing techniques can offer the ability to fine tune the physiochemical properties of such structures. Furthermore, surface modifications can be studied using peptides, growth factors and conductive polymers to further enhance the scaffold's functionality and support cell growth and proliferation.

Therefore, acquiring knowledge from every step of the cellulose-based 3D porous scaffold process is critical to commercialize them as potential biomaterials for tissue engineering.

**Author Contributions:** Conceptualization, A.M., R.M.; methodology, A.M.; resources, A.M.; data curation, A.M., R.M.; writing—original draft preparation, A.M.; writing—review and editing, A.M., R.M. and J.L.; supervision, R.M. and J.L.; project administration, A.M.; All authors have read and agreed to the published version of the manuscript.

**Funding:** This research received no external funding.

**Conflicts of Interest:** The authors declare no conflict of interest.

## References

1. Burg, K.J.L.; Porter, S.; Kellam, J.F. Biomaterial developments for bone tissue engineering. *Biomaterials* **2000**, *21*, 2347–2359. [[CrossRef](#)]
2. Ko, H.F.; Sfeir, C.; Kumta, P.N. Novel synthesis strategies for natural polymer and composite biomaterials as potential scaffolds for tissue engineering. *Philos. Trans. R. Soc. A Math. Phys. Eng. Sci.* **2010**, *368*, 1981–1997. [[CrossRef](#)]
3. Yannas, I.V. *Tissue and Organ Regeneration in Adults: Extension of the Paradigm to Several Organs*; Springer: Berlin/Heidelberg, Germany, 2014.
4. Takei, T.; Okonogi, A.; Tateno, K.; Kimura, A.; Kojima, S.; Yazaki, K.; Miura, K.I. The effects of the side chains of hydrophobic aliphatic amino acid residues in an amphipathic polypeptide on the formation of  $\alpha$  helix and its association. *J. Biochem.* **2006**, *139*, 271–278. [[CrossRef](#)]
5. Supp, D.M.; Boyce, S.T. Engineered skin substitutes: Practices and potentials. *Clin. Dermatol.* **2005**, *23*, 403–412. [[CrossRef](#)]
6. Mitrousis, N.; Fokina, A.; Shoichet, M.S. Biomaterials for cell transplantation. *Nat. Rev. Mater.* **2018**, *3*, 441–456. [[CrossRef](#)]
7. Bacakova, L.; Pajorova, J.; Bacakova, M.; Skogberg, A.; Kallio, P.; Kolarova, K.; Svorcik, V. Versatile application of nanocellulose: From industry to skin tissue engineering and wound healing. *Nanomaterials* **2019**, *9*, 164. [[CrossRef](#)]
8. Ashraf, R.; Sofi, H.S.; Akram, T.; Rather, H.A.; Abdal-hay, A.; Shabir, N.; Vasita, R.; Alrokayan, S.H.; Khan, H.A.; Sheikh, F.A. Fabrication of multifunctional cellulose/TiO<sub>2</sub>/Ag composite nanofibers scaffold with antibacterial and bioactivity properties for future tissue engineering applications. *J. Biomed. Mater. Res. Part A* **2020**, *108*, 947–962. [[CrossRef](#)]
9. Kang, X.; Xie, Y.; Powell, H.M.; Lee, L.J.; Belury, M.A.; Lannutti, J.J.; Kniss, D.A. Adipogenesis of murine embryonic stem cells in a three-dimensional culture system using electrospun polymer scaffolds. *Biomaterials* **2007**, *28*, 450–458. [[CrossRef](#)]
10. Mandal, B.B.; Kundu, S.C. Osteogenic and adipogenic differentiation of rat bone marrow cells on non-mulberry and mulberry silk gland fibroin 3D scaffolds. *Biomaterials* **2009**, *30*, 5019–5030. [[CrossRef](#)]
11. Wang, J.; Zong, C.; Shi, D.; Wang, W.; Shen, D.; Liu, L.; Tong, X.; Zheng, Q.; Gao, C. Hepatogenic engineering from human bone marrow mesenchymal stem cells in porous polylactic glycolic acid scaffolds under perfusion culture. *J. Tissue Eng. Regen. Med.* **2012**, *6*, 29–39. [[CrossRef](#)]
12. Kuboki, Y.; Jin, Q.; Takita, H. Geometry of carriers controlling phenotypic expression in BMP-induced osteogenesis and chondrogenesis. *J. Bone Jt. Surg. Am.* **2001**, *83 Pt 2*. [[CrossRef](#)]
13. Mygind, T.; Stiehler, M.; Baatrup, A.; Li, H.; Zou, X.; Flyvbjerg, A.; Kassem, M.; Bünger, C. Mesenchymal stem cell ingrowth and differentiation on coralline hydroxyapatite scaffolds. *Biomaterials* **2007**, *28*, 1036–1047. [[CrossRef](#)]
14. Shor, L.; Güçeri, S.; Chang, R.; Gordon, J.; Kang, Q.; Hartsock, L.; An, Y.; Sun, W. Precision extruding deposition (PED) fabrication of polycaprolactone (PCL) scaffolds for bone tissue engineering. *Biofabrication* **2009**, *1*. [[CrossRef](#)]
15. Lien, S.M.; Ko, L.Y.; Huang, T.J. Effect of pore size on ECM secretion and cell growth in gelatin scaffold for articular cartilage tissue engineering. *Acta Biomater.* **2009**, *5*, 670–679. [[CrossRef](#)]
16. Yannas, I.V.; Lee, E.; Orgill, D.P.; Skrabut, E.M.; Murphy, G.F. Synthesis and characterization of a model extracellular matrix that induces partial regeneration of adult mammalian skin. *Proc. Natl. Acad. Sci. USA* **1989**, *86*, 933–937. [[CrossRef](#)]
17. Rnjak-Kovacina, J.; Wise, S.G.; Li, Z.; Maitz, P.K.M.; Young, C.J.; Wang, Y.; Weiss, A.S. Tailoring the porosity and pore size of electrospun synthetic human elastin scaffolds for dermal tissue engineering. *Biomaterials* **2011**, *32*, 6729–6736. [[CrossRef](#)]
18. Akay, G.; Birch, M.A.; Bokhari, M.A. Microcellular polyHIPE polymer supports osteoblast growth and bone formation in vitro. *Biomaterials* **2004**, *25*, 3991–4000. [[CrossRef](#)]
19. Artel, A.; Mehdizadeh, H.; Chiu, Y.C.; Brey, E.M.; Cinar, A. An agent-based model for the investigation of neovascularization within porous scaffolds. *Tissue Eng. Part A* **2011**, *17*, 2133–2141. [[CrossRef](#)]

20. Matinfar, M.; Mesgar, A.S.; Mohammadi, Z. Evaluation of physicochemical, mechanical and biological properties of chitosan/carboxymethyl cellulose reinforced with multiphasic calcium phosphate whisker-like fibers for bone tissue engineering. *Mater. Sci. Eng. C* **2019**, *100*, 341–353. [[CrossRef](#)]
21. Bhardwaj, N.; Chouhan, D.; Mandal, B.B. 3D functional scaffolds for skin tissue engineering. *Funct. 3D Tissue Eng. Scaffolds* **2018**, 345–365. [[CrossRef](#)]
22. Barrios, E.; Fox, D.; Li Sip, Y.Y.; Catarata, R.; Calderon, J.E.; Azim, N.; Afrin, S.; Zhang, Z.; Zhai, L. Nanomaterials in advanced, high-performance aerogel composites: A review. *Polymers* **2019**, *11*, 726. [[CrossRef](#)]
23. Şahin, İ.; Özbakır, Y.; İnönü, Z.; Ulker, Z.; Erkey, C. Kinetics of Supercritical Drying of Gels. *Gels* **2017**, *4*, 3. [[CrossRef](#)]
24. Baldino, L.; Cardea, S.; Reverchon, E. Natural aerogels production by supercritical gel drying. *Chem. Eng. Trans.* **2015**. [[CrossRef](#)]
25. Nieto-Suárez, M.; López-Quintela, M.A.; Lazzari, M. Preparation and characterization of crosslinked chitosan/gelatin scaffolds by ice segregation induced self-assembly. *Carbohydr. Polym.* **2016**. [[CrossRef](#)]
26. Sola, A.; Bertacchini, J.; D'Avella, D.; Anselmi, L.; Maraldi, T.; Marmiroli, S.; Messori, M. Development of solvent-casting particulate leaching (SCPL) polymer scaffolds as improved three-dimensional supports to mimic the bone marrow niche. *Mater. Sci. Eng. C* **2019**, *96*, 153–165. [[CrossRef](#)]
27. Ganesan, K.; Budtova, T.; Ratke, L.; Gurikov, P.; Baudron, V.; Preibisch, I.; Niemyer, P.; Smirnova, I.; Milow, B. Review on the production of polysaccharide aerogel particles. *Materials* **2018**, *11*, 2144. [[CrossRef](#)]
28. Gunathilake, T.M.S.U.; Ching, Y.C.; Chuah, C.H. Enhancement of curcumin bioavailability using nanocellulose reinforced chitosan hydrogel. *Polymers* **2017**, *9*, 64. [[CrossRef](#)]
29. Gauvin, R.; Chen, Y.C.; Lee, J.W.; Soman, P.; Zorlutuna, P.; Nichol, J.W.; Bae, H.; Chen, S.; Khademhosseini, A. Microfabrication of complex porous tissue engineering scaffolds using 3D projection stereolithography. *Biomaterials* **2012**, *33*, 3824–3834. [[CrossRef](#)]
30. Madou, M.J. *Fundamentals of Microfabrication: The Science of Miniaturization*; CRC Press: Boca Raton, FL, USA, 2002.
31. Chen, W.; Xu, Y.; Liu, Y.; Wang, Z.; Li, Y.; Jiang, G.; Mo, X.; Zhou, G. Three-dimensional printed electrospun fiber-based scaffold for cartilage regeneration. *Mater. Des.* **2019**, *179*, 107886. [[CrossRef](#)]
32. Jun, I.; Han, H.S.; Edwards, J.R.; Jeon, H. Electrospun fibrous scaffolds for tissue engineering: Viewpoints on architecture and fabrication. *Int. J. Mol. Sci.* **2018**, *19*, 745. [[CrossRef](#)]
33. El-Naggar, M.E.; Othman, S.I.; Allam, A.A.; Morsy, O.M. Synthesis, drying process and medical application of polysaccharide-based aerogels. *Int. J. Biol. Macromol.* **2020**, *145*, 1115–1128. [[CrossRef](#)]
34. Jovic, T.H.; Kungwengwe, G.; Mills, A.C.; Whitaker, I.S. Plant-Derived Biomaterials: A Review of 3D Bioprinting and Biomedical Applications. *Front. Mech. Eng.* **2019**, *5*. [[CrossRef](#)]
35. Markstedt, K.; Mantas, A.; Tournier, I.; Martínez Ávila, H.; Hägg, D.; Gatenholm, P. 3D bioprinting human chondrocytes with nanocellulose-alginate bioink for cartilage tissue engineering applications. *Biomacromolecules* **2015**, *16*, 1489–1496. [[CrossRef](#)]
36. Lavoine, N.; Bergström, L. Nanocellulose-based foams and aerogels: Processing, properties, and applications. *J. Mater. Chem. A* **2017**, *5*, 16105–16117. [[CrossRef](#)]
37. Fereshteh, Z. Freeze-drying technologies for 3D scaffold engineering. In *Functional 3D Tissue Engineering Scaffolds: Materials, Technologies, and Applications*; Woodhead Publishing: Cambridge, UK, 2018; pp. 151–174, ISBN 9780081009802.
38. Campodoni, E.; Heggset, E.B.; Rashad, A.; Ramírez-Rodríguez, G.B.; Mustafa, K.; Syverud, K.; Tampieri, A.; Sandri, M. Polymeric 3D scaffolds for tissue regeneration: Evaluation of biopolymer nanocomposite reinforced with cellulose nanofibrils. *Mater. Sci. Eng. C* **2019**, *94*, 867–878. [[CrossRef](#)]
39. Morais, A.R.D.V.; Alencar, É.D.N.; Xavier Júnior, F.H.; Oliveira, C.M.D.; Marcelino, H.R.; Barratt, G.; Fessi, H.; Egito, E.S.T.D.; Elaissari, A. Freeze-drying of emulsified systems: A review. *Int. J. Pharm.* **2016**, *503*, 102–114. [[CrossRef](#)]
40. Mirab, F.; Eslamian, M.; Bagheri, R. Fabrication and characterization of a starch-based nanocomposite scaffold with highly porous and gradient structure for bone tissue engineering. *Biomed. Phys. Eng. Express* **2018**, *4*. [[CrossRef](#)]
41. Nasri-Nasrabadi, B.; Mehrasa, M.; Rafienia, M.; Bonakdar, S.; Behzad, T.; Gavanji, S. Porous starch/cellulose nanofibers composite prepared by salt leaching technique for tissue engineering. *Carbohydr. Polym.* **2014**, *108*, 232–238. [[CrossRef](#)]

42. Varshney, D.; Singh, M. History of Lyophilization. In *Lyophilized Biologics and Vaccines*; Springer: Berlin/Heidelberg, Germany, 2015.
43. Long, L.Y.; Weng, Y.X.; Wang, Y.Z. Cellulose aerogels: Synthesis, applications, and prospects. *Polymers* **2018**, *8*, 623. [[CrossRef](#)]
44. Vasanthan, K.S.; Subramaniam, A.; Krishnan, U.M.; Sethuraman, S. Influence of 3D porous galactose containing PVA/gelatin hydrogel scaffolds on three-dimensional spheroidal morphology of hepatocytes. *J. Mater. Sci. Mater. Med.* **2015**, *26*. [[CrossRef](#)]
45. Lim, J.Y.; Lim, D.G.; Kim, K.H.; Park, S.K.; Jeong, S.H. Effects of annealing on the physical properties of therapeutic proteins during freeze drying process. *Int. J. Biol. Macromol.* **2018**, *107*, 730–740. [[CrossRef](#)]
46. Yan, J.; Wu, T.; Ding, Z.; Li, X. Preparation and characterization of carbon nanotubes/chitosan composite foam with enhanced elastic property. *Carbohydr. Polym.* **2016**, *136*, 1288–1296. [[CrossRef](#)]
47. Jiménez-Saelices, C.; Seantier, B.; Cathala, B.; Grohens, Y. Effect of freeze-drying parameters on the microstructure and thermal insulating properties of nanofibrillated cellulose aerogels. *J. Sol-Gel Sci. Technol.* **2017**, *84*, 475–485. [[CrossRef](#)]
48. Asuncion, M.C.T.; Goh, J.C.H.; Toh, S.L. Anisotropic silk fibroin/gelatin scaffolds from unidirectional freezing. *Mater. Sci. Eng. C* **2016**, *67*, 646–656. [[CrossRef](#)]
49. Liu, H.; Nakagawa, K.; Chaudhary, D.; Asakuma, Y.; Tadé, M.O. Freeze-dried macroporous foam prepared from chitosan/xanthan gum/montmorillonite nanocomposites. *Chem. Eng. Res. Des.* **2011**, *89*, 2356–2364. [[CrossRef](#)]
50. Lederman, M. Stage II Carcinoma of the Cervix. *Proc. R. Soc. Med.* **1976**, *69*, 859. [[CrossRef](#)]
51. Ribeiro, D.M.L.; Júnior, A.R.C.; de Macedo, G.H.R.V.; Chagas, V.L.; Silva, L.D.S.; Cutrim, B.D.S.; Santos, D.M.; Soares, B.L.L.; Zagnignan, A.; de Miranda, R.D.C.M.; et al. Polysaccharide-based formulations for healing of skin-related wound infections: Lessons from animal models and clinical trials. *Biomolecules* **2020**, *10*, 63. [[CrossRef](#)]
52. Zhao, S.; Malfait, W.J.; Guerrero-Alburquerque, N.; Koebel, M.M.; Nyström, G. Biopolymer Aerogels and Foams: Chemistry, Properties, and Applications. *Angew. Chem. Int. Ed.* **2018**, *57*, 7580–7608. [[CrossRef](#)]
53. Muthuraj, R.; Grohens, Y.; Seantier, B. Mechanical and thermal insulation properties of elium acrylic resin/cellulose nanofiber based composite aerogels. *Nano-Struct. Nano-Objects* **2017**, *12*, 68–76. [[CrossRef](#)]
54. Bai, X.; Gao, M.; Syed, S.; Zhuang, J.; Xu, X.; Zhang, X.Q. Bioactive hydrogels for bone regeneration. *Bioact. Mater.* **2018**, *3*, 401–417. [[CrossRef](#)]
55. Shen, X.; Shamshina, J.L.; Berton, P.; Gurau, G.; Rogers, R.D. Hydrogels based on cellulose and chitin: Fabrication, properties, and applications. *Green Chem.* **2015**, *18*, 53–75. [[CrossRef](#)]
56. Ki, C.S.; Baek, D.H.; Gang, K.D.; Lee, K.H.; Um, I.C.; Park, Y.H. Characterization of gelatin nanofiber prepared from gelatin-formic acid solution. *Polymer* **2005**, *46*, 5094–5102. [[CrossRef](#)]
57. Panzavolta, S.; Gioffrè, M.; Focarete, M.L.; Gualandi, C.; Foroni, L.; Bigi, A. Electrospun gelatin nanofibers: Optimization of genipin cross-linking to preserve fiber morphology after exposure to water. *Acta Biomater.* **2011**, *7*, 1702–1709. [[CrossRef](#)]
58. Powell, H.M.; Supp, D.M.; Boyce, S.T. Influence of electrospun collagen on wound contraction of engineered skin substitutes. *Biomaterials* **2008**, *29*, 834–843. [[CrossRef](#)]
59. Li, X.; Xiao, Z.; Han, J.; Chen, L.; Xiao, H.; Ma, F.; Hou, X.; Li, X.; Sun, J.; Ding, W.; et al. Promotion of neuronal differentiation of neural progenitor cells by using EGFR antibody functionalized collagen scaffolds for spinal cord injury repair. *Biomaterials* **2013**, *34*, 5107–5116. [[CrossRef](#)]
60. Lynn, A.K.; Yannas, I.V.; Bonfield, W. Antigenicity and immunogenicity of collagen. *J. Biomed. Mater. Res. Part B Appl. Biomater* **2004**, *71*, 343–354. [[CrossRef](#)]
61. Mogoşanu, G.D.; Grumezescu, A.M. Natural and synthetic polymers for wounds and burns dressing. *Int. J. Pharm.* **2014**, *463*, 127–136. [[CrossRef](#)]
62. Afewerki, S.; Sheikhi, A.; Kannan, S.; Ahadian, S.; Khademhosseini, A. Gelatin-polysaccharide composite scaffolds for 3D cell culture and tissue engineering: Towards natural therapeutics. *Bioeng. Transl. Med.* **2019**, *4*, 96–115. [[CrossRef](#)]
63. Mirtaghavi, A.; Baldwin, A.; Tanideh, N.; Zarei, M.; Muthuraj, R.; Cao, Y.; Zhao, G.; Geng, J.; Jin, H.; Luo, J. Crosslinked porous three-dimensional cellulose nanofibers-gelatin biocomposite scaffolds for tissue regeneration. *Int. J. Biol. Macromol.* **2020**, *164*, 1949–1959. [[CrossRef](#)]
64. Alissandratos, A.; Halling, P.J. Enzymatic acylation of starch. *Bioresour. Technol.* **2012**, *115*, 41–47. [[CrossRef](#)]

65. Quraishi, S.; Martins, M.; Barros, A.A.; Gurikov, P.; Raman, S.P.; Smirnova, I.; Duarte, A.R.C.; Reis, R.L. Novel non-cytotoxic alginate–lignin hybrid aerogels as scaffolds for tissue engineering. *J. Supercrit. Fluids* **2015**, *105*, 1–8. [[CrossRef](#)]
66. Jonoobi, M.; Harun, J.; Mathew, A.P.; Oksman, K. Mechanical properties of cellulose nanofiber (CNF) reinforced polylactic acid (PLA) prepared by twin screw extrusion. *Compos. Sci. Technol.* **2010**, *70*, 1742–1747. [[CrossRef](#)]
67. Syverud, K. Tissue Engineering Using Plant-Derived Cellulose Nanofibrils (CNF) as Scaffold Material. In *Nanocelluloses: Their Preparation, Properties, and Applications*; American Chemical Society: Washington, DC, USA, 2017; pp. 171–189.
68. Jiménez-Saelices, C.; Seantier, B.; Cathala, B.; Grohens, Y. Spray freeze-dried nanofibrillated cellulose aerogels with thermal superinsulating properties. *Carbohydr. Polym.* **2017**, *157*, 105–113. [[CrossRef](#)]
69. Ferreira, F.V.; Otoni, C.G.; De France, K.J.; Barud, H.S.; Lona, L.M.F.; Cranston, E.D.; Rojas, O.J. Porous nanocellulose gels and foams: Breakthrough status in the development of scaffolds for tissue engineering. *Mater. Today* **2020**, *37*, 126–141. [[CrossRef](#)]
70. Gaihre, B.; Jayasuriya, A.C. Fabrication and characterization of carboxymethyl cellulose novel microparticles for bone tissue engineering. *Mater. Sci. Eng. C* **2016**, *69*, 733–743. [[CrossRef](#)]
71. Ninan, N.; Muthiah, M.; Park, I.K.; Elain, A.; Thomas, S.; Grohens, Y. Pectin/carboxymethyl cellulose/microfibrillated cellulose composite scaffolds for tissue engineering. *Carbohydr. Polym.* **2013**, *98*, 877–885. [[CrossRef](#)]
72. Nechyporchuk, O.; Belgacem, M.N.; Bras, J. Production of cellulose nanofibrils: A review of recent advances. *Ind. Crop. Prod.* **2016**, *93*, 2–25. [[CrossRef](#)]
73. Nishino, T.; Matsuda, I.; Hirao, K. All-cellulose composite. *Macromolecules* **2004**, *37*, 7683–7687. [[CrossRef](#)]
74. Moreira, S.; Silva, N.B.; Almeida-Lima, J.; Rocha, H.A.O.; Medeiros, S.R.B.; Alves, C.; Gama, F.M. BC nanofibres: In vitro study of genotoxicity and cell proliferation. *Toxicol. Lett.* **2009**, *189*, 235–241. [[CrossRef](#)]
75. Dong, S.; Hirani, A.A.; Colacino, K.R.; Lee, Y.W.; Roman, M. Cytotoxicity and Cellular Uptake of Cellulose Nanocrystals. *Nano Life* **2012**, *2*, 1241006. [[CrossRef](#)]
76. Dugan, J.M.; Gough, J.E.; Eichhorn, S.J. Bacterial cellulose scaffolds and cellulose nanowhiskers for tissue engineering. *Nanomedicine* **2013**, *8*, 287–298. [[CrossRef](#)]
77. Vandamme, E.J.; De Baets, S.; Vanbaelen, A.; Joris, K.; De Wulf, P. Improved production of bacterial cellulose and its application potential. *Polym. Degrad. Stab.* **1998**, *59*, 93–99. [[CrossRef](#)]
78. Kamel, S. Nanotechnology and its applications in lignocellulosic composites, a mini review. *Express Polym. Lett.* **2007**, *1*, 546–575. [[CrossRef](#)]
79. Klemm, D.; Kramer, F.; Moritz, S.; Lindström, T.; Ankerfors, M.; Gray, D.; Dorris, A. Nanocelluloses: A new family of nature-based materials. *Angew. Chem. Int. Ed.* **2011**, *50*, 5438–5466. [[CrossRef](#)]
80. Frone, A.N.; Panaitescu, D.M.; Nicolae, C.A.; Gabor, A.R.; Trusca, R.; Casarica, A.; Stanescu, P.O.; Baci, D.D.; Salageanu, A. Bacterial cellulose sponges obtained with green cross-linkers for tissue engineering. *Mater. Sci. Eng. C* **2020**, *110*. [[CrossRef](#)]
81. Gutiérrez-Hernández, J.M.; Escobar-García, D.M.; Escalante, A.; Flores, H.; González, F.J.; Gatenholm, P.; Toriz, G. In vitro evaluation of osteoblastic cells on bacterial cellulose modified with multi-walled carbon nanotubes as scaffold for bone regeneration. *Mater. Sci. Eng. C* **2017**, *75*, 445–453. [[CrossRef](#)]
82. Pértile, R.; Moreira, S.; Andrade, F.; Domingues, L.; Gama, M. Bacterial cellulose modified using recombinant proteins to improve neuronal and mesenchymal cell adhesion. *Biotechnol. Prog.* **2012**, *28*, 526–532. [[CrossRef](#)]
83. Torgbo, S.; Sukyai, P. Bacterial cellulose-based scaffold materials for bone tissue engineering. *Appl. Mater. Today* **2018**, *11*, 34–49. [[CrossRef](#)]
84. Laskowski, J.; Milow, B.; Ratke, L. The effect of embedding highly insulating granular aerogel in cellulosic aerogel. *J. Supercrit. Fluids* **2015**, *106*. [[CrossRef](#)]
85. Sirvio, J.; Hyvakkko, U.; Liimatainen, H.; Niinimäki, J.; Hormi, O. Periodate oxidation of cellulose at elevated temperatures using metal salts as cellulose activators. *Carbohydr. Polym.* **2011**, *83*, 1293–1297. [[CrossRef](#)]
86. Lu, T.; Li, Q.; Chen, W.; Yu, H. Composite aerogels based on dialdehyde nanocellulose and collagen for potential applications as wound dressing and tissue engineering scaffold. *Compos. Sci. Technol.* **2014**, *94*, 132–138. [[CrossRef](#)]

87. Saito, T.; Kuramae, R.; Wohler, J.; Berglund, L.A.; Isogai, A. An ultrastrong nanofibrillar biomaterial: The strength of single cellulose nanofibrils revealed via sonication-induced fragmentation. *Biomacromolecules* **2013**, *14*, 248–253. [[CrossRef](#)]
88. Baker, B.M.; Trappmann, B.; Wang, W.Y.; Sakar, M.S.; Kim, I.L.; Shenoy, V.B.; Burdick, J.A.; Chen, C.S. Cell-mediated fibre recruitment drives extracellular matrix mechanosensing in engineered fibrillar microenvironments. *Nat. Mater.* **2015**, *14*, 1262–1268. [[CrossRef](#)]
89. Muthuraj, R.; Sachan, A.; Castro, M.; Feller, J.F.; Seantier, B.; Grohens, Y. Vapor and pressure sensors based on cellulose nanofibers and carbon nanotubes aerogel with thermoelectric properties. *J. Renew. Mater.* **2018**, *6*, 277–287. [[CrossRef](#)]
90. Rashad, A.; Mustafa, K.; Heggset, E.B.; Syverud, K. Cytocompatibility of Wood-Derived Cellulose Nanofibril Hydrogels with Different Surface Chemistry. *Biomacromolecules* **2017**, *18*, 1238–1248. [[CrossRef](#)]
91. Naderi, A.; Lindström, T.; Sundström, J. Carboxymethylated nanofibrillated cellulose: Rheological studies. *Cellulose* **2014**, *21*, 1561–1571. [[CrossRef](#)]
92. Hickey, R.J.; Pelling, A.E. Cellulose biomaterials for tissue engineering. *Front. Bioeng. Biotechnol.* **2019**, *7*. [[CrossRef](#)]
93. Krontiras, P.; Gatenholm, P.; Hagg, D.A. Adipogenic differentiation of stem cells in three-dimensional porous bacterial nanocellulose scaffolds. *J. Biomed. Mater. Res. Part B Appl. Biomater.* **2015**, *103*, 195–203. [[CrossRef](#)]
94. Li, V.C.F.; Dunn, C.K.; Zhang, Z.; Deng, Y.; Qi, H.J. Direct Ink Write (DIW) 3D Printed Cellulose Nanocrystal Aerogel Structures. *Sci. Rep.* **2017**, *7*. [[CrossRef](#)]
95. Håkansson, K.M.O.; Henriksson, I.C.; de la Peña Vázquez, C.; Kuzmenko, V.; Markstedt, K.; Enoksson, P.; Gatenholm, P. Solidification of 3D Printed Nanofibril Hydrogels into Functional 3D Cellulose Structures. *Adv. Mater. Technol.* **2016**, *1*. [[CrossRef](#)]
96. Cai, H.; Sharma, S.; Liu, W.; Mu, W.; Liu, W.; Zhang, X.; Deng, Y. Aerogel microspheres from natural cellulose nanofibrils and their application as cell culture scaffold. *Biomacromolecules* **2014**, *15*, 2540–2547. [[CrossRef](#)]
97. Isogai, A.; Saito, T.; Fukuzumi, H. TEMPO-oxidized cellulose nanofibers. *Nanoscale* **2011**, *3*, 71–85. [[CrossRef](#)]
98. Bhattacharya, M.; Malinen, M.M.; Lauren, P.; Lou, Y.R.; Kuisma, S.W.; Kanninen, L.; Lille, M.; Corlu, A.; Guguen-Guillouzo, C.; Ikkala, O.; et al. Nanofibrillar cellulose hydrogel promotes three-dimensional liver cell culture. *J. Control. Release* **2012**, *164*, 291–298. [[CrossRef](#)]
99. Vartiainen, J.; Pöhler, T.; Sirola, K.; Pylkkänen, L.; Alenius, H.; Hokkinen, J.; Tapper, U.; Lahtinen, P.; Kapanen, A.; Putkisto, K.; et al. Health and environmental safety aspects of friction grinding and spray drying of microfibrillated cellulose. *Cellulose* **2011**, *18*, 775–786. [[CrossRef](#)]
100. Alexandrescu, L.; Syverud, K.; Gatti, A.; Chinga-Carrasco, G. Cytotoxicity tests of cellulose nanofibril-based structures. *Cellulose* **2013**, *20*, 1765–1775. [[CrossRef](#)]
101. Liu, Y.; Sui, Y.; Liu, C.; Liu, C.; Wu, M.; Li, B.; Li, Y. A physically crosslinked polydopamine/nanocellulose hydrogel as potential versatile vehicles for drug delivery and wound healing. *Carbohydr. Polym.* **2018**, *188*, 27–36. [[CrossRef](#)]
102. Liu, J.; Cheng, F.; Grénman, H.; Spoljaric, S.; Seppälä, J.; Eriksson, J.E.; Willför, S.; Xu, C. Development of nanocellulose scaffolds with tunable structures to support 3D cell culture. *Carbohydr. Polym.* **2016**, *148*, 259–271. [[CrossRef](#)]
103. Kilpeläinen, P.; Kitunen, V.; Pranovich, A.; Ilvesniemi, H.; Willför, S. Pressurized hot water flow-through extraction of birch sawdust with acetate pH buffer. *BioResources* **2013**, *8*, 5202–5218. [[CrossRef](#)]
104. Shvedova, A.A.; Kisin, E.R.; Yanamala, N.; Farcas, M.T.; Menas, A.L.; Williams, A.; Fournier, P.M.; Reynolds, J.S.; Gutkin, D.W.; Star, A.; et al. Gender differences in murine pulmonary responses elicited by cellulose nanocrystals. *Part. Fibre Toxicol.* **2016**, *13*. [[CrossRef](#)]
105. Alvarez, M.M.; Liu, J.C.; Trujillo-de Santiago, G.; Cha, B.H.; Vishwakarma, A.; Ghaemmaghami, A.M.; Khademhosseini, A. Delivery strategies to control inflammatory response: Modulating M1–M2 polarization in tissue engineering applications. *J. Control. Release* **2016**, *240*, 349–363. [[CrossRef](#)]
106. Naseri, N.; Poirier, J.M.; Girandon, L.; Fröhlich, M.; Oksman, K.; Mathew, A.P. 3-Dimensional porous nanocomposite scaffolds based on cellulose nanofibers for cartilage tissue engineering: Tailoring of porosity and mechanical performance. *RSC Adv.* **2016**, *6*, 5999–6007. [[CrossRef](#)]
107. Pei, Y.; Ye, D.; Zhao, Q.; Wang, X.; Zhang, C.; Huang, W.; Zhang, N.; Liu, S.; Zhang, L. Effectively promoting wound healing with cellulose/gelatin sponges constructed directly from a cellulose solution. *J. Mater. Chem. B* **2015**, *3*, 7518–7528. [[CrossRef](#)]

108. Carlström, I.E.; Rashad, A.; Campodoni, E.; Sandri, M.; Syverud, K.; Bolstad, A.I.; Mustafa, K. Cross-linked gelatin-nanocellulose scaffolds for bone tissue engineering. *Mater. Lett.* **2020**, *264*, 127326. [[CrossRef](#)]
109. Ghafari, R.; Jonoobi, M.; Amirabad, L.M.; Oksman, K.; Taheri, A.R. Fabrication and characterization of novel bilayer scaffold from nanocellulose based aerogel for skin tissue engineering applications. *Int. J. Biol. Macromol.* **2019**, *136*, 796–803. [[CrossRef](#)]
110. Wu, J.; Zheng, Y.; Wen, X.; Lin, Q.; Chen, X.; Wu, Z. Silver nanoparticle/bacterial cellulose gel membranes for antibacterial wound dressing: Investigation in vitro and in vivo. *Biomed. Mater.* **2014**, *9*. [[CrossRef](#)]
111. Hosseini, H.; Zirakjou, A.; Goodarzi, V.; Mousavi, S.M.; Khonakdar, H.A.; Zamanlui, S. Lightweight aerogels based on bacterial cellulose/silver nanoparticles/polyaniline with tuning morphology of polyaniline and application in soft tissue engineering. *Int. J. Biol. Macromol.* **2020**, *152*, 57–67. [[CrossRef](#)]
112. Schneider, C.; Gordon, O.N.; Edwards, R.L.; Luis, P.B. Degradation of Curcumin: From Mechanism to Biological Implications. *J. Agric. Food Chem.* **2015**, *63*, 7606–7614. [[CrossRef](#)]
113. Sahu, A.N. Nanotechnology in herbal medicines and cosmetics. *Int. J. Res. Ayurveda Pharm.* **2013**, *4*, 472–474. [[CrossRef](#)]
114. Shefa, A.A.; Sultana, T.; Park, M.K.; Lee, S.Y.; Gwon, J.G.; Lee, B.T. Curcumin incorporation into an oxidized cellulose nanofiber-polyvinyl alcohol hydrogel system promotes wound healing. *Mater. Des.* **2020**, *186*, 108313. [[CrossRef](#)]
115. Yin, N.; Du, R.; Zhao, F.; Han, Y.; Zhou, Z. Characterization of antibacterial bacterial cellulose composite membranes modified with chitosan or chitooligosaccharide. *Carbohydr. Polym.* **2020**, *229*. [[CrossRef](#)]
116. Ao, H.; Jiang, W.; Nie, Y.; Zhou, C.; Zong, J.; Liu, M.; Liu, X.; Wan, Y. Engineering quaternized chitosan in the 3D bacterial cellulose structure for antibacterial wound dressings. *Polym. Test.* **2020**, *86*, 106490. [[CrossRef](#)]
117. Fan, X.; Li, Y.; Li, X.; Wu, Y.; Tang, K.; Liu, J.; Zheng, X.; Wan, G. Injectable antibacterial cellulose nanofiber/chitosan aerogel with rapid shape recovery for noncompressible hemorrhage. *Int. J. Biol. Macromol.* **2020**, *154*, 1185–1193. [[CrossRef](#)]

**Publisher's Note:** MDPI stays neutral with regard to jurisdictional claims in published maps and institutional affiliations.



© 2020 by the authors. Licensee MDPI, Basel, Switzerland. This article is an open access article distributed under the terms and conditions of the Creative Commons Attribution (CC BY) license (<http://creativecommons.org/licenses/by/4.0/>).